



Structural and morphological characterization of silver nanoparticles intruded mineral trioxide aggregate admixture as a chair-side restorative medicament: an *in vitro* experimental study

H. Murali Rao¹ , Rajkumar Krishnan² , Chitra Shivalingam³ , Ramya Ramadoss^{4,*} 

¹Conservative Dentistry and Endodontics, DA Pandu Memorial RV Dental College, Bengaluru, India

²Department of Oral Pathology, SRM Dental College, Chennai, India

³Department of Prosthodontics, Saveetha Dental College, Saveetha Institute of Science and Technology, Chennai, India

⁴Department of Oral Biology, Saveetha Dental College, Saveetha Institute of Science and Technology, Chennai, India

ABSTRACT

Objectives: The aim of this study was to create a rapid admixture of mineral trioxide aggregate (MTA) and silver nanoparticles (AgNPs) for chairside use in clinical settings to remediate the challenges associated with root canal treatment and pulp capping.

Methods: Synthesized AgNPs at ratios of 10 and 25% were added to commercially available MTA to create an admixture. The admixture was subjected to structural and morphological assessment using X-ray diffraction analysis (XRD), Fourier transform infrared (FT-IR) analysis, Raman spectroscopy, and scanning electron microscopy. Antioxidant activity was measured using the hydroxyl radical scavenging assay. A significance level of 0.05 was applied to determine statistical differences.

Results: The addition of AgNPs decreased the carbonate peak intensity in XRD and FT-IR. The rod-like morphology of MTA was changed to a flake-like morphology with the addition of AgNPs. Antibacterial efficacy enhanced proportionally with the augmentation of AgNPs concentration.

Conclusions: The creation of rapid admixture of MTA and AgNPs during chairside use in clinical settings can deliver beneficial characteristics of enhanced morphological features favoring mineralization and profound antibacterial effects to overcome the challenges associated with root canal treatment and pulp capping.

Keywords: Mineral trioxide aggregate; Nanoparticles; Pulp capping; Silver

Received: July 21, 2024 Revised: December 1, 2024 Accepted: December 3, 2024

Citation

Rao HM, Krishnan R, Shivalingam C, Ramadoss R. Structural and morphological characterization of silver nanoparticles intruded mineral trioxide aggregate admixture as a chair-side restorative medicament: an *in vitro* experimental study. Restor Dent Endod 2025;50(3):e30.

*Correspondence to

Ramya Ramadoss, MDS, PhD

Department of Oral Pathology, Saveetha Dental College, Saveetha Institute of Science and Technology, 162 Poonamallee High Road, Chennai 600077, Tamil Nadu, India

Email: dr.ramya268@gmail.com

© 2025 The Korean Academy of Conservative Dentistry

This is an Open Access article distributed under the terms of the Creative Commons Attribution Non-Commercial License (<https://creativecommons.org/licenses/by-nc/4.0/>) which permits unrestricted non-commercial use, distribution, and reproduction in any medium, provided the original work is properly cited.

INTRODUCTION

The primary objective of endodontic therapy is to eradicate all microorganisms within the root canal and effectively seal any potential communication channels between the pulp and surrounding tissues [1,2]. Among currently available root-end filling materials, mineral trioxide aggregate (MTA) plays a pivotal role in restorative dentistry with improved biocompatibility and sealing ability [3]. MTA is a bioceramic with primary components consisting of tricalcium silicate, dicalcium silicate, and tricalcium aluminate. Key indications of MTA are root-end filling, pulp capping, pulpotomy, root perforation repair, apexification, and regenerative endodontics [4].

The antimicrobial property of MTA is limited, and MTA exhibits synergistic antimicrobial properties when mixed with other substances or medications frequently employed in endodontic treatment, such as chlorhexidine or antibiotics. These combinations have demonstrated improved antibacterial effectiveness [5]. Incorporation of silver (Ag) into MTA could also enhance the antibacterial characteristics, increasing its efficacy in treating bacterial infections in dental applications [6,7]. The antibacterial properties of silver have been widely acknowledged for their effectiveness against a wide range of pathogens found in endodontic infections. The inclusion of silver in MTA offers supplementary advantages in endodontic treatment that include reduced microleakage, extended longevity, and enhanced biocompatibility [8].

Literature has revealed that combining silver nanoparticles (AgNPs) with MTA is an attractive option as a novel retrograde filling, with increased effectiveness of AgNPs in inhibiting the growth of *Enterococcus faecalis* [9,10]. Similarly, MTA and calcium-enriched mixture incorporated with AgNPs had a significant effect on bacteria associated with dental infections [10]. Further, the morphology of the mineral composites also influenced the material's efficiency in endodontics. The elongated form of rod-like particles enhanced infiltration into the adjacent tissues or biomaterial matrices, thus strengthening the interactions between MTA particles and the surrounding environment, favoring apatite formation [9,11]. Despite promising results, there is no product

that has been translated into clinical use.

The creation of a rapid admixture of MTA and AgNPs for chairside use in clinical settings could serve as a practical way to achieve the beneficial characteristics of enhanced mineralization and antioxidant effects. Such synergistic actions are crucial to remediate the challenges associated with root canal treatment and pulp capping. This study aimed to enhance the properties of three different commercially available MTAs, including MTA White, MTA Plus, and MTA Repair, by incorporating AgNPs. Additionally, structural, morphological, and antibacterial characteristics were evaluated.

METHODS

Synthesis of silver nanoparticles

AgNPs were synthesized utilizing a chemical reduction approach [12]. Constituents of reactive materials were produced in double-distilled water. For the standard procedure, a solution containing 50 mL of silver nitrate (AgNO_3) with a concentration of 1×10^{-3} M was heated until it reached its boiling point. A volume of 5 mL of 1% sodium borohydride (NaBH_4) was added gradually to this mixture. The solution was vigorously agitated during this procedure and heated until a discernible change in color (light brown) occurred. Eventually, it was extracted in powder form (50–80 nm) from the heating component and agitated until it reached the ambient temperature of 100°C for 12 hours [13].

Silver nanoparticles intruded mineral trioxide aggregate admixture

Physical mixing of varying ratios of AgNPs (10% and 25%) with different brands of MTA White (Angelus, Londrina, Brazil), MTA Plus (Prevest DenPro, Jammu, India), and MTA Insta Repair (Raman Research Products, Bangalore, India) was carried out. The numbers '10' and '25' indicate the content (wt%) of AgNPs. Samples were run in triplicate in similar experimental conditions with a total sample size of $n = 27$ (9 samples per group). An admixture of 3 g was dispensed on a paper pad and mixed with sterile water in the ratio of 0.26, using a plastic spatula for a duration of 1 to 3 minutes till a thick paste-like consistency was achieved. The mixture was separated into portions and allowed to set for 30 minutes.

Characterization

MTA-AgNP admixture was analyzed for X-ray diffraction patterns to assess the crystalline phases with the wavelength Cu K α (Bruker D8 Advance; Bruker, Karlsruhe, Germany). Functional group properties were analyzed through Raman spectroscopy (ALPHA300 RA; WITec, Ulm, Germany). Morphological and elemental analyses were done using scanning electron microscopy (SEM) (JSM-IT 800; JEOL, Tokyo, Japan). The samples were loaded onto the stub using adhesive tape and sputter-coated with platinum. Imaging of the sample was done at a scale of 1 μ m.

Antioxidant activity

The hydroxyl radical scavenging assay was done by taking a known volume of the test sample [14]. The mixture was made as a 10 mM stock solution and incubated for 30 minutes at 37°C to allow hydroxyl radicals to react. Following the addition of 1 mL of 10% trichloroacetic acid and 1 mL of 1% thiobarbituric acid solution, the reaction was then stopped by heating the mixture in a boiling water bath for 30 minutes to generate a pink complex denoting the endpoint. Following cooling, a spectrophotometer was used to measure the absorbance at 532 nm. The hydroxyl radical scavenging activity was then calculated as a percentage using the following formula: % scavenging activity = [(control absorbance - sample absorbance) / control absorbance] \times 100. The results were validated by including the appropriate controls and replicates [15].

Statistical analysis

Statistical analysis was performed to evaluate differences in antioxidant potential based on the percentage of reduction achieved across three groups at varying concentrations. A one-way analysis of variance (ANOVA) test was performed, as the data followed a normal distribution, had similar variances, and were independent measurements. ANOVA was used to calculate the *F*-statistic. A significance level of $p < 0.05$ was applied to determine statistically meaningful differences. The analysis was performed using IBM SPSS version 24 (IBM Corp, Armonk, NY, USA).

RESULTS

Structural analysis

MTA contains calcium silicate as a major component along with traces of zirconia, bismuth, and phosphate. In the case of X-ray diffraction dominant Ca₃SiO₅ crystalline phase was noted along with the diffracted peaks of CaCO₃.

Fourier transform infrared (FT-IR) spectra demonstrated in Figure 1 revealed silica (460 cm⁻¹) and phosphate (575 cm⁻¹) vibrations, indicating the presence of bioceramics. The Ca₃SiO₅ crystalline phase was evinced as the primary phase along with CaCO₃. When compared to MTA White samples, some noise peaks were observed, intense 29° peaks indicating dominant calcium carbonate were also noted. The CaCO₃ peak appears suppressed in the presence of AgNPs. Compared to MTA White samples, deep silica and phosphate vibrations were noted in other samples, along with sharp crystalline peaks exhibited in X-ray diffraction analysis (XRD) [11,16].

Morphological analysis

Imaging of the samples was done using SEM at 1 μ m as illustrated in Figure 2. Tiny rod-shaped morphology was evident in the pure MTA White sample. After introducing silver into MTA White sample, AgNPs displayed flake-like morphology. Further, rods are joined together to form an interconnected bunch-rod appearance in MTA Plus samples. Infusion of silver on bunched rod appearances resulted in flakes and sheet-like morphology. Increasing the concentration of small spherical silver particles with the integration of bunched rods was perceptible. Non-homogeneous spiky rods, as well as elongated sheet-like morphology, were noted in pure MTA Insta Repair. Further addition of silver into these rods and sheets revealed integrated flake-like morphology.

Antioxidant activity

The hydroxyl radical scavenging assay, revealed in Figures 3 and 4, demonstrated the ability of the samples to neutralize harmful hydroxyl radicals. Results demonstrated that all samples with AgNPs exhibited antioxidant activity. The inter-group comparison of antioxidant

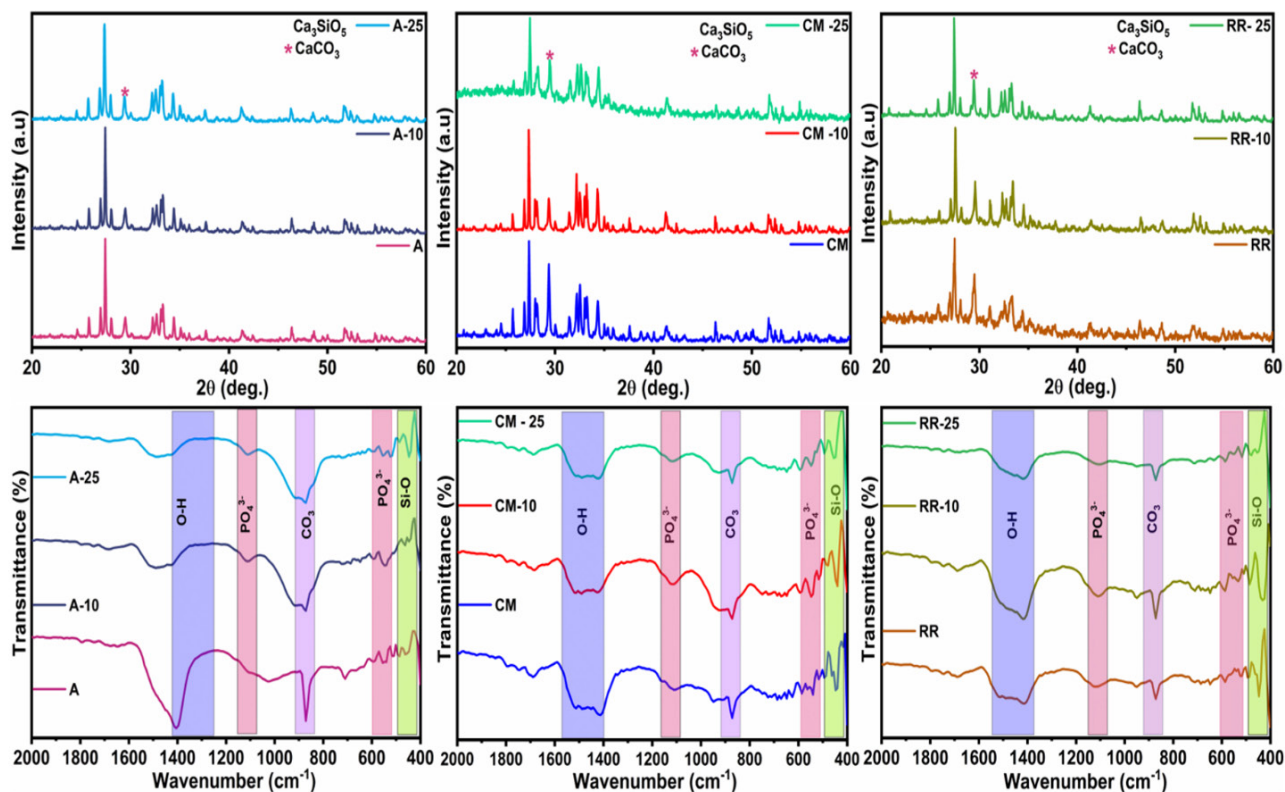


Figure 1. X-ray diffraction (XRD) and Fourier transform infrared (FT-IR) spectra of the tested materials. (A) XRD spectra of pure MTA White (denoted as 'A'), A-10, and A-25. (B) XRD spectra of MTA Plus (denoted as 'CM'), CM-10, and CM-25. (C) XRD spectra of pure MTA Insta Repair (denoted as 'RR'), RR-10, and RR-25. (D) FT-IR spectra of A, A-10, and A-25. (E) FT-IR spectra of CM, CM-10, and CM-25. (F) FT-IR spectra of RR, RR-10, and RR-25. *10 and 25 represent the contents (mg) of silver nanoparticles in pure base materials, including A, RR, and CM, respectively. MTA White: Angelus, Londrina, Brazil; MTA Plus: Prevest DenPro, Jammu, India; MTA Insta Repair: Raman Research Products, Bangalore, India.

activity of the three materials (MTA White, MTA Plus, and MTA Insta Repair) was analyzed using one-way ANOVA to assess the differences in reduction percentage with different concentrations of AgNPs (pure; 10 mg and 25 mg). Statistical significance was observed in all materials, with F -statistics of 221.71 ($p = 2.38 \times 10^{-6}$) for MTA White, 160.33 ($p = 6.20 \times 10^{-6}$) for MTA Plus, and 72.33 ($p = 6.32 \times 10^{-5}$) for MTA Insta Repair. Further, intragroup comparison was done using repeated measures ANOVA. Results revealed statistically significant differences within each dental cement group. In MTA White group, F -statistic was 221.71 with a p -value of 2.38×10^{-6} 2.38×10^{-6} . MTA Plus group exhibited significant variation with an F -statistic of 160.33 and a p -value of 6.20×10^{-6} . MTA Insta Repair group also demonstrated significant differences, with an F -statistic of 72.33 and a p -value of 6.32×10^{-5} . The results revealed that AgNPs

exhibit a significant hydroxyl radical scavenging ability.

DISCUSSION

MTA has emerged as a versatile material for root-end filling and pulp-capping agents due to its bioactive and biocompatible properties. Additional properties like good sealing ability, setting properties, and antimicrobial potential have made it the most sought-after bioactive material in endodontics [17]. However, the antimicrobial property of MTA is potentially less; enhancing the antibacterial property of MTA is of profound importance, considering the increasing evidence of persistent periapical infections. The addition of AgNPs to the MTA matrix has been reported by multiple studies to improve antimicrobial properties. The lower concentrations of AgNPs have also been demonstrated to impart sufficient

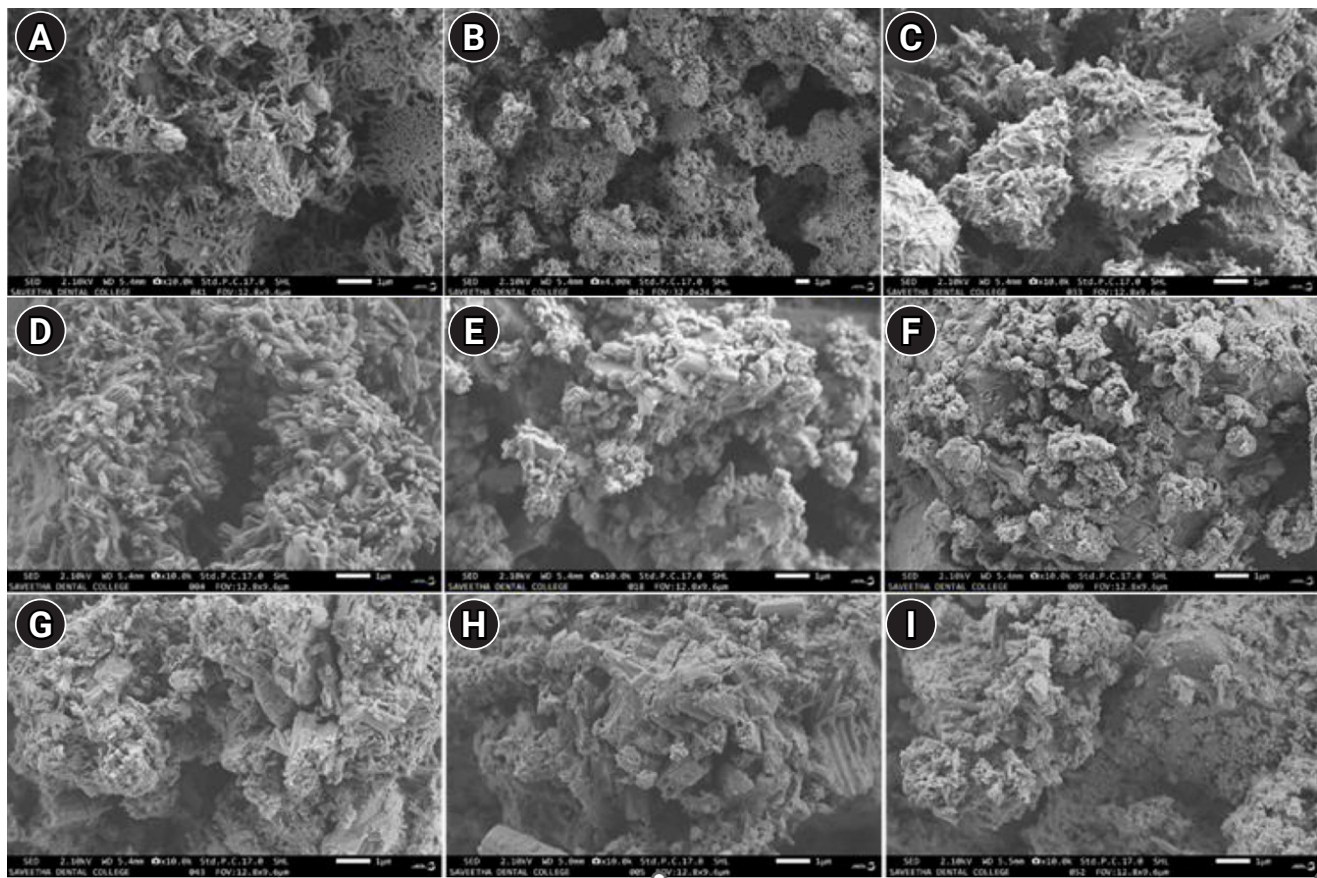


Figure 2. Scanning electron microscopy (SEM) images showing the morphological characteristics of the tested materials. (A) Pure MTA White (denoted as 'A'). (B) A + 10 mg silver nanoparticles (AgNPs). (C) A + 25 mg AgNPs. (D) Pure MTA Plus (denoted as 'CM'). (E) CM + 10 mg AgNPs. (F) CM + 25 mg AgNPs. (G) Pure MTA Insta Repair (denoted as 'RR'). (H) RR + 10 mg AgNPs. (I) RR + 25 mg AgNPs. MTA White: Angelus, Londrina, Brazil; MTA Plus: Prevest DenPro, Jammu, India; MTA Insta Repair: Raman Research Products, Bangalore, India.

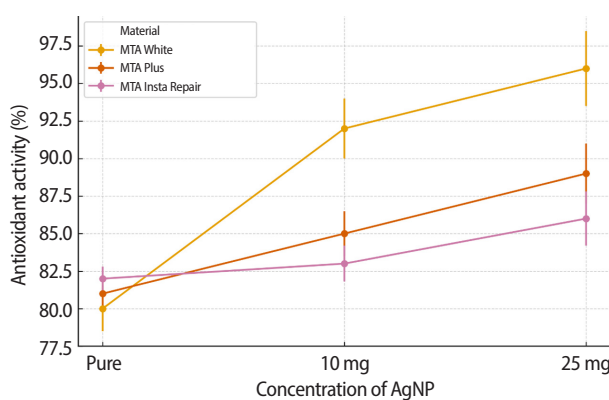


Figure 3. Intergroup comparison of the antioxidant activity of MTA White group, MTA Plus group, and MTA Insta Repair group. AgNP, silver nanoparticle. MTA White: Angelus, Londrina, Brazil; MTA Plus: Prevest DenPro, Jammu, India; MTA Insta Repair: Raman Research Products, Bangalore, India.

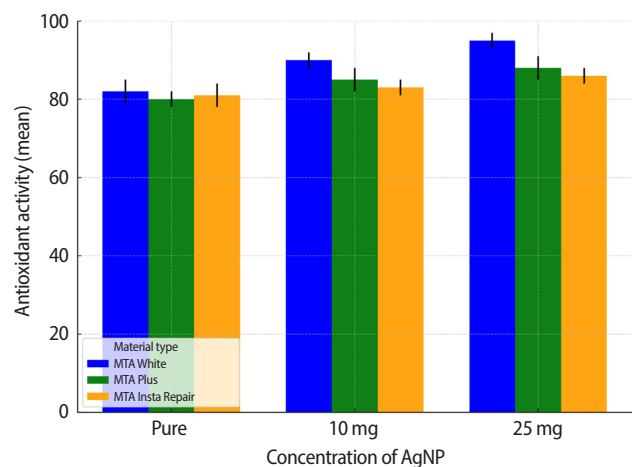


Figure 4. Intra-group comparison of the antioxidant activity. AgNP, silver nanoparticle. MTA White: Angelus, Londrina, Brazil; MTA Plus: Prevest DenPro, Jammu, India; MTA Insta Repair: Raman Research Products, Bangalore, India.

antimicrobial properties while maintaining the biocompatibility and mechanical integrity of MTA [9]. Although the results have shown promise, there are currently no products that are available for clinical use. Developing a quick and easy mixture of MTA and AgNPs for use directly in the dental office as an admixture could be a practical approach to benefit from the advantages. The current study focused on validating the structure and morphology of an MTA mixture infused with AgNPs.

AgNPs have been a versatile source to increase antimicrobial activity. Their addition tends to alter the crystalline configuration and phase transitions favorable to render antimicrobial properties [11,12]. Our study results indicated the presence of silver in all samples with prominent peaks due to the crystalline nature of silver, in addition to strong vibration of silica and blended phosphate vibrations, despite being a non-homogenized preparation. Calcium silicate as well as calcium carbonate diffraction peaks were observed through the XRD patterns. After the impregnation of silver, the noise peaks turned into sharp peaks due to the crystalline nature of silver. Sharp peaks are indicative of strong vibration of silica and blended phosphate vibration. After the addition of AgNPs, all three samples exhibited a decrease in intensity in carbonate peaks both in XRD as well as FT-IR. AgNPs caused a reduction of carbonate peak intensity both in XRD as well as FT-IR due to potential interaction or interference between the AgNPs and the carbonate molecules. Adsorption of carbonate ions to the surface of AgNPs resulted in reduced availability for the detection of carbonate molecules during analysis. This adsorption process may change the vibrational or diffractive characteristics of the carbonate ions, thus decreasing their intensities at peaks. Additionally, distinct silica and phosphate vibrations and the presence of intense crystalline peaks indicate a significant impact of AgNPs on the crystal structure of the samples. These characteristics of AgNPs in the presence of calcium-based composites are similar to other studies, irrespective of the method of synthesis [18]. Further, results were also indicative of the changes in the crystal configuration in terms of lattice parameters, crystal morphology, or orientation, suggestive of an intricate interplay between AgNPs and MTA matrix leading to fundamental re-arrangement of the crystal lattice. Cal-

cium silicate and calcium carbonate diffraction peaks in the XRD patterns could be ascribed to a crystalline phase transition due to a complex molecular interaction between the AgNPs and the MTA matrix. AgNPs do not show changes in crystalline configuration with minimal concentration; prominent alterations are due to the higher concentration in the prepared admixture [19].

Structural changes evidenced by SEM revealed a rod-like morphology of MTA. The addition of spherical-shaped AgNPs resulted in an alteration of rod orientation with flake-like morphology. In most samples, MTA explicated a rod-like morphology. The morphology has an impactful role in the mineralization and durability of the restoration. It is hypothesized that, along with mineral components, crystal structure plays an enormous role in tubule occlusion. MTA sealers predominantly exhibit rod-like morphology addition of AgNPs resulted in an alteration of rod orientation with flake-like morphology. The rods attached to the flakes of AgNPs were observed at all angles. Complete adherence of rods to the particles is ascribed to the nominal size of the rod-like structure [11]. The transformation from a rod-like to a flake-like morphology in MTA involves intricate molecular-level changes that influence crystal growth. The incorporation of AgNPs may modify the nucleation kinetics, crystallographic orientations, or surface energies, thereby influencing the formation of flake-like structures with a different molecular arrangement [19].

AgNPs have a profound hydroxyl radical scavenging ability, due to a high surface area to volume ratio, favoring interaction with free radicals. Antioxidant activity was evident in all samples with AgNPs. This substantiates the advantage of enhanced ability to scavenge hydroxyl radicals and increase the probability of interactions with free radicals. This characteristic is beneficial in the management of inflammatory environments that persist in periapical infections [16]. Additionally, AgNPs also have the prowess to augment the efficacy of other antioxidants to provide a synergistic effect, which is crucial in the regulation of oxidative stress. However, studies also indicate that antioxidant efficacy can vary with different formulations [20]. Variations in antioxidant activity among the MTA types were observed in the study. MTA White exhibited improved efficacy when

compared to other products; however, the differences were minimal. This could be attributed to the similar composition of the key ingredients like calcium silicate, bismuth oxide, calcium sulfate, and calcium hydroxide.

These findings underscore the potential clinical applications of AgNPs in dental and biomedical fields, where oxidative stress is implicated in inflammation and tissue damage. Importantly, when used at appropriate concentrations, AgNPs display favorable biocompatibility, making them suitable for medical applications without adversely affecting cell viability. Together, these attributes position AgNPs as valuable components in formulations aimed at combating oxidative stress and promoting health.

The incorporation of AgNPs into the MTA matrix confers several benefits, like enhanced antioxidant properties, improved sealing ability, potentially enhanced bioactivity, and sustainability [18]. The sustained release of calcium and hydroxyl ions from the MTA-AgNPs admixture is expected to promote a favorable microenvironment for tissue regeneration and antimicrobial activity [9]. However, the incorporation of AgNPs into the MTA matrix may also pose potential challenges, such as the potential impact on the material's physical and mechanical properties, as well as the possible cytotoxic effects of AgNPs at high concentrations [20]. Therefore, a careful balance between the benefits and the biocompatibility of the MTA-AgNPs admixture must be established through comprehensive *in vitro* and *in vivo* evaluations.

CONCLUSIONS

The structural and morphological characterization of AgNPs-intruded MTA admixture as a chairside restorative medicament holds promise for enhanced antioxidant properties, improved clinical outcomes, and sustainability. However, further research is needed to optimize the formulation and ensure the safety and efficacy of this novel MTA-based material.

CONFLICT OF INTEREST

No potential conflict of interest relevant to this article was reported.

FUNDING/SUPPORT

The authors have no financial relationships relevant to this article to disclose.

AUTHOR CONTRIBUTIONS

Conceptualization: Ramadoss R, Rao HM, Krishnan R. Data curation, Investigation, Methodology: Ramadoss R, Shivalingam C. Formal analysis, Software, Validation: Shivalingam C. Visualization, Resources: Rao HM. Project administration, Supervision: Krishnan R. Writing - original draft: Ramadoss R. Writing - review & editing: Rao HM, Ramadoss R. All authors read and approved the final manuscript.

DATA SHARING STATEMENT

The datasets are not publicly available but are available from the corresponding author upon reasonable request.

REFERENCES

1. Narayanan LL, Vaishnavi C. Endodontic microbiology. J Conserv Dent 2010;13:233-239.
2. Wong J, Manoil D, Näsman P, Belibasakis GN, Neelakantan P. Microbiological aspects of root canal infections and disinfection strategies: an update review on the current knowledge and challenges. Front Oral Health 2021;2:672887.
3. von Arx T. Apical surgery: a review of current techniques and outcome. Saudi Dent J 2011;23:9-15.
4. Saxena P, Gupta SK, Newaskar V. Biocompatibility of root-end filling materials: recent update. Restor Dent Endod 2013;38:119-127.
5. Camilleri J. The chemical composition of mineral trioxide aggregate. J Conserv Dent 2008;11:141-143.
6. Nasri S, Afkhami F. Efficacy of MTA modified by nanosilver for the prevention of coronal leakage. Open Dent J 2021;15:204-209.
7. Lee MY, Yoon HW, Kim KM, Kwon JS. Antibacterial efficacy and osteogenic potential of mineral trioxide aggregate-based retrograde filling material incorporated with silver nanoparticle and calcium fluoride. J Dent Sci 2024;19:1783-1791.
8. Camilleri J, Sorrentino F, Damidot D. Investigation of the hydration and bioactivity of radiopacified tricalcium silicate cement, Biodentine and MTA Angelus. Dent Mater 2013;29:580-593.
9. Jonaidi-Jafari N, Izadi M, Javidi P. The effects of silver nanoparticles on antimicrobial activity of ProRoot mineral trioxide aggregate (MTA) and calcium enriched mixture (CEM). J Clin Exp Dent 2016;8:e22-e26.

10. Zakrzewski W, Dobrzyński M, Zawadzka-Knefel A, Luboński A, Dobrzyński W, Janecki M, *et al.* Nanomaterials application in endodontics. *Materials (Basel)* 2021;14:5296.
11. Çınar Ç, Odabaş M, Gürel MA, Baldağ I. The effects of incorporation of silver-zeolite on selected properties of mineral trioxide aggregate. *Dent Mater J* 2013;32:872-876.
12. Ghatole K, Patil A, Giriyappa RH, Singh TV, Jyotsna SV, Rairam S. Evaluation of antibacterial efficacy of MTA with and without additives like silver zeolite and chlorhexidine. *J Clin Diagn Res* 2016;10:ZC11-ZC14.
13. Quintero-Quiroz C, Acevedo N, Zapata-Giraldo J, Botero LE, Quintero J, Zárate-Triviño D, *et al.* Optimization of silver nanoparticle synthesis by chemical reduction and evaluation of its antimicrobial and toxic activity. *Biomater Res* 2019;23:27.
14. Khuda F, Jamil M, Khalil AA, Ullah R, Ullah N, Naureen F, *et al.* Assessment of antioxidant and cytotoxic potential of silver nanoparticles synthesized from root extract of Reynoutria japonica Houtt. *Arab J Chem* 2022;15:104327.
15. Cervino G, Fiorillo L, Spagnuolo G, Bramanti E, Laino L, Lauritano F, *et al.* Interface between MTA and dental bond-ing agents: scanning electron microscope evaluation. *J Int Soc Prev Community Dent* 2017;7:64-68.
16. Kim S, Choi JE, Choi J, Chung KH, Park K, Yi J, *et al.* Oxidative stress-dependent toxicity of silver nanoparticles in human hepatoma cells. *Toxicol In Vitro* 2009;23:1076-1084.
17. Sarkar NK, Anand P, Moiseyeva R, Ritwik R. A modified Portland Cement for dental use: its interaction with simulated oral environment. *Trans Indian Ceram Soc* 2003;62:200-204.
18. Inkret S, Ćurlin M, Smokrović K, Kalčec N, Peranić N, Maltar-Strmečki N, *et al.* Can differently stabilized silver nanoparticles modify calcium phosphate precipitation? *Materials (Basel)* 2023;16:1764.
19. Padmanabhan VP, Sivashanmugam P, Kulandaivelu R, Sagadevan S, Sridevi B, Govindasamy R, *et al.* Biosynthesised silver nanoparticles loading onto biphasic calcium phosphate for antibacterial and bone tissue engineering applications. *Antibiotics (Basel)* 2022;11:1780.
20. Raju R, Prasad AS, S RK. Anti-inflammatory and antioxidant activity of neem and kirata-induced silver nanoparticles against oral biofilm: an in vitro study. *Cureus* 2024;16:e67708.